NANO LETTERS

pubs.acs.org/NanoLett

Slow Hot-Carrier Relaxation in Colloidal Graphene Quantum Dots

Mallory L. Mueller, Xin Yan, Bogdan Dragnea, and Liang-shi Li*

Department of Chemistry, Indiana University, Bloomington, Indiana 47405, United States

ABSTRACT Reducing hot-carrier relaxation rates is of great significance in overcoming energy loss that fundamentally limits the efficiency of solar energy utilization. Semiconductor quantum dots are expected to have much slower carrier cooling because the spacing between their discrete electronic levels is much larger than phonon energy. However, the slower carrier cooling is difficult to observe due to the existence of many competing relaxation pathways. Here we show that carrier cooling in colloidal graphene quantum dots can be 2 orders of magnitude slower than in bulk materials, which could enable harvesting of hot charge carriers to improve the efficiency of solar energy conversion.

KEYWORDS Graphene, quantum dots, energy relaxation, carrier cooling, quantum confinement

When the size of a semiconductor crystal is reduced to approach the exciton Bohr radius of the bulk material, the limited volume significantly modifies electron distribution, resulting in size-dependent properties such as bandgap and energy relaxation dynamics.[1−3] This phenomenon, known as "quantum confinement", has been investigated in many semiconductor materials and led to practical applications such as bioimaging, lasing, photovoltaics, and light-emitting diodes. For these electro-optical applications of quantum dots, relaxation of high excited states (or cooling of hot carriers) is of central importance and thus has been extensively studied.[4−6] Because of the large electronic energy spacing in quantum confined systems in comparison with phonon frequencies, phonon-assisted relaxation between discrete electronic states requires emission of multiple phonons to conserve energy. Since the phonon-assisted relaxation is the primary mechanism for carrier cooling in bulk semiconductors, it was expected that carrier cooling in quantum dots should be significantly slower than in bulk semiconductors because of the low probability of multiphonon processes (i.e., "phonon bottleneck").[5,7] In reality, however, in quantum dots there exist alternative relaxation mechanisms efficient enough to cause subpicosecond carrier cooling that is not significantly slower than that in bulk materials.[8,9] In particular, hot electrons could relax rapidly by transferring energy to holes, which often have a greater effective mass and thus smaller energy spacing, through Auger-like processes followed by phonon-assisted relaxation[10,11] or nonadiabatic channels involving surface ligands.[12,13] Trap states[14,15] in the quantum dots and high-frequency vibrational modes in surface ligands[16] provide additional relaxation pathways to promote rapid carrier cooling. It has been demonstrated that by carefully designing multiple layers of heterostructures around colloidal CdSe quantum dots and suppressing these pathways, the lifetimes of hot carriers could be increased by 3 orders of magnitude up to 1 ns.[9] With this approach, electrons and holes were spatially separated by the heterostructures to reduce their energy transfer. Epitaxial growth of the heterostructures and use of weakly IR-absorbing surface ligands further removed the trap states and coupling with ligand vibrations.

Herein we report on the observation that indicates remarkably slow carrier cooling in colloidal graphene quantum dots.[17−19] Comparing with quantum dots of other semiconductors such as CdSe or PbSe, colloidal graphene quantum dots have features that could naturally suppress the hot-carrier relaxation pathways in addition to the phonon-assisted ones. Having symmetric linear energy dispersion relations in both valence band and conduction band near the band edges makes equal effective masses for both electrons and holes,[20] eliminating the Auger-like electron−hole energy transfer pathways for carrier cooling. With well-controlled carbon chemistry, we can make graphenes that consist of carbon atoms with only sp^2-hybridization and perfectly passivate their edges with hydrogen atoms, so that the quantum dots are free of trap states. In addition, all the chemical bonds in the colloidal graphene quantum dots can be precisely controlled to have small mid-IR transition dipole moments so that they do not strongly couple to the electrons of the graphenes.[9] Our experimental studies on the carrier relaxation dynamics of colloidal graphene quantum dots indeed show the absence of fast relaxation pathways so that lifetimes of hot carriers up to hundreds of picoseconds could be readily obtained. The slower carrier cooling, together with the small dielectric constant in graphene and thus greater carrier−carrier Columbic interaction, makes the graphene quantum dots an interesting system to investigate alternative relaxation pathways such as hot electron transfer or multiexciton generation for improving efficiency of photovoltaic devices.[21]

* To whom correspondence should be addressed. Email: li23@indiana.edu.
Received for review: 08/2/2010
Published on Web: 12/02/2010

© 2011 American Chemical Society

DOI: 10.1021/nl102712x | *Nano Lett.* **2011,** *11,* 56–60

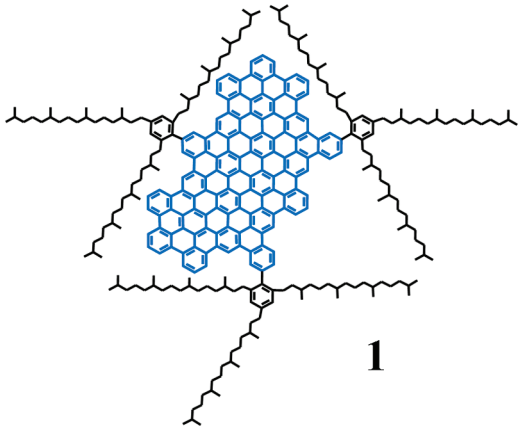

FIGURE 1. Structure of graphene quantum dot 1 studied in this work. The graphene core is marked in blue, and the solubilizing 2′,4′,6′-trialkyl phenyl groups are marked black. The graphene core is terminated with hydrogen atoms (not shown) on the edges except at the positions connecting to the solubilizing groups.

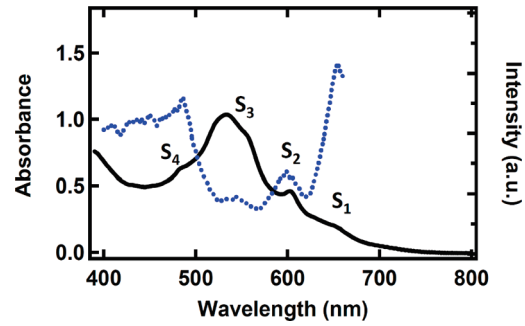

FIGURE 2. Absorption (solid curve, left axis) and fluorescence excitation spectrum (dotted curve, right axis) of 1 studied in this work. S_{1-4} labels the final singlet states responsible for the transitions. The excitation spectrum was measured by monitoring the emission at 670 nm.

The graphene quantum dots we studied contain 132 conjugated carbon atoms (**1** in Figure 1; the graphene core is marked in blue). They were synthesized with a recently developed solution-chemistry approach, so that the quantum dots contain a graphene core with perfect size uniformity solubilized by three flexible 2′,4′,6′-trialkyl phenyl groups (marked in black).[17,18] The steric constraints on the edges of the graphene forces the trialkyl phenyl groups to twist from the plane of the graphene, creating a three-dimensional cage that effectively prevents the quantum dots from aggregating.[17] As a result, the quantum dots can be dispersed in various solvents, and we can study their ensemble properties unhindered by aggregation or substrate effects.[22]

Previous studies on graphite indicated that the strong coupling between optical phonons and charge carriers leads to subpicosecond cooling of hot carriers.[23,24] In bulk graphene epitaxially grown on solid substrates, it was observed that carrier-phonon scattering leads to cooling within less than two picoseconds.[25,26] To compare the hot-carrier relaxation dynamics in **1** with that in the bulk materials, the graphene quantum dots were studied in solution with ultrafast transient absorption spectroscopy at room temperature. For the experiments, the quantum dots were dispersed in toluene with a concentration of ~10 μM, and the solution was bubbled with argon for at least 10 min immediately before the measurements. In the transient absorption experiments, the solution is pumped with laser pulses with 400 nm wavelength, 150 fs pulse width, 10 nm bandwidth, and a repetition rate of 250 kHz. The pump beam is the second harmonic of the 800 nm output of a Ti:sapphire regenerative amplifier (RegA, Coherent) seeded by a mode-locked oscillator (Mira, Coherent) at 76 MHz. A fraction of the 800 nm output was used to pump an optical parametric amplifier (OPA), from which the output with tunable wavelength (500−700 nm) was used for the probe. For measurements of relaxation decay, the OPA output was split into a reference and a probe beam with the reference beam arriving at a fixed time before the probe. The time delay between the pump and the probe was continuously scanned by passing the pump beam through a delay line of adjustable lengths. A mechanical chopper was used to modulate the pump beam at 780 Hz. The differential signal between the reference and the probe beams was measured with a pair of balanced silicon photodiodes (100 kHz bandwidth, New Focus, model 2307) and detected with a lock-in amplifier (Stanford Research System, SR 830) at the modulation frequency. The energy density of each pump and probe pulse incident onto the sample was ~50 and ~1 nJ/mm^2, respectively, to make sure that each quantum dot can absorb at most one photon from each pump pulse and that the transmitted probe beam intensity was within the linear response range of the photodiodes.

The absorption spectrum of **1** in toluene is shown in Figure 2, which appears continuous because of vibronic broadening and the small energy spacing between the excited electronic states. Each of the transition bands in the spectrum is denoted with the corresponding final states S_{1-4} (from ground state S_0), with S representing the singlet states and S_1 the lowest excited singlet state. Fluorescence excitation spectrum (Figure 2, dotted curve) shows that the absorption at wavelengths shorter than 490 nm is due to transitions to continuum electronic states, to which the quantum dots were initially excited with the 400 nm pump beam in our transient absorption experiments. The different trends in the absorption and the excitation spectra at various wavelengths are because the quantum dots at states S_2 and S_3 have significant probabilities to relax into triplet states.[22] Since in the graphene quantum dots carrier−carrier interactions and quantum-size energy are much greater than the zero bandgap of bulk graphene, in their excited states (including S_1-S_4) the coupling between electron states and hole states have to be considered. The excitonic effects have been shown to play important roles in determining the optical properties of carbon nanotubes[27] as well as bulk graphene and nanoribbons.[28,29] In quantum dot **1**, the small size and reduced dimensionality further enhance carrier−carrier interactions. By assuming a dielectric constant of unity for

© 2011 American Chemical Society

DOI: 10.1021/nl102712x | Nano Lett. 2011, 11, 56–60

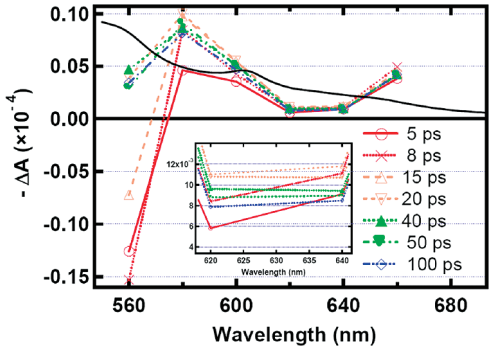

FIGURE 3. Transient absorption (TA) signals of 1 between 560 to 660 nm at various pump−probe time delays. The inset is the zoom-in of the signals at 620 and 640 nm. Only for 560 nm did we observe an induced absorption signal. The black, solid curve is the absorption spectrum (arbitrary unit).

graphene,[30] we can estimate the electron−hole Columbic interaction $E_C \sim -[e^2/(4\pi\varepsilon_o a)] \sim -1$ eV, where $a \sim 1$ nm is the radius of **1**. In addition, the quantum-size energy $E_q \sim (\nu_F h)/(2a) \sim 2$ eV, where $\nu_F \approx 10^6 m/s$, is the Fermi velocity in graphene.[31] Therefore, in the excited states of the quantum dots (S_{1-4}) various electron or hole states are strongly mixed. Consequently in the relaxation of hot carriers the evolution of electrons and holes are correlated and cannot be treated independently as in CdSe quantum dots.[32]

Absorption bleaching in **1** subsequent to pulsed irradiation at 400 nm was observed at all probed wavelengths. In Figure 3 we show the transient absorption (TA) signals at wavelengths probed between 560 to 660 nm with a 20 nm interval at various pump−probe time delays. Among the six wavelengths we have studied, five showed only bleaching and the subsequent recovery. The signal at 560 nm showed an induced absorption transition, presumably because of excited quantum dots being further excited, generating either an exciton of higher energy or two excitons. Its exact origin will be investigated in the future.

At each of the wavelengths we have probed, the bleaching recovery dynamics can be described with two exponential components, of which the faster one has a time constant independent of wavelength and the slower one wavelength-dependent. Figures 4 shows the time traces of the TA signals at 560, 600, 640, and 660 nm, corresponding to $S_0 \rightarrow S_3$, $S_0 \rightarrow S_2$, $S_0 \rightarrow S_1$ (blue edge) and $S_0 \rightarrow S_1$ (red edge) transitions, respectively. In Figure 4 we also show the best global biexponential fits for all the traces, assuming the time constant of the faster component being equal for all the wavelengths. This leads to the faster component of 18 ± 3 ps and the slower one ranging from approximately 100 ps to nanoseconds (Figure 4).

On the basis of the mechanisms for light-induced bleaching in quantum dots, that is, Columbic exciton−exciton interactions or state filling,[32] we can attribute the slower time constants in the bleaching recovery traces to the lifetimes of the excited states with excitation energies corresponding to those of the probe beams. Exciton−exciton

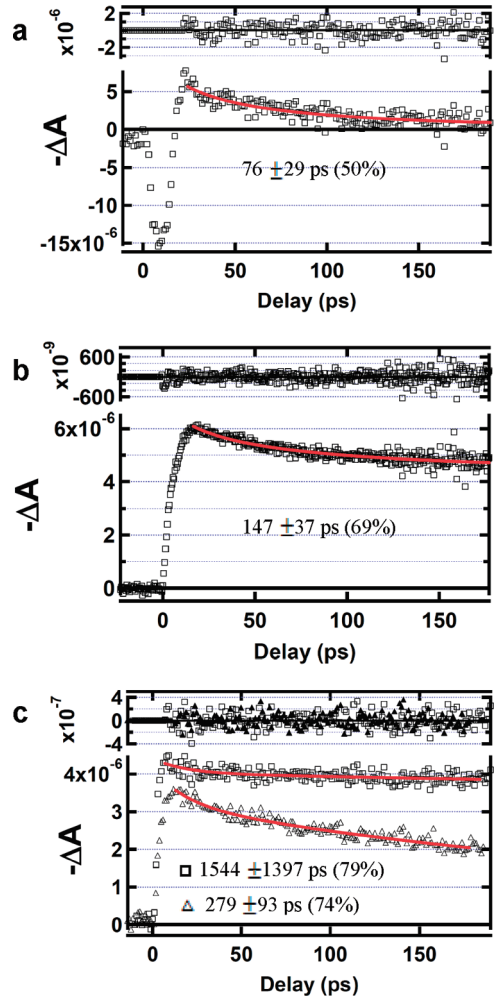

FIGURE 4. Transient absorption signals probed at (a) 560, (b) 600, (c) 640 (×3, triangles) and 660 nm (squares) with the best global biexponential fits (red curves) for the bleaching recovery. For the fitting, the traces were assumed to have the same faster component, which was obtained to be 18 ± 3 ps. The numbers in the panels are the obtained time constants for the slower components with their weight percentage in the parentheses. The residues for the fits are also shown on the top of each panel. For the signals at 580 and 620 nm (in Supporting Information), the time constants of the slower components are 185 ± 51 (10%) and 251 ± 106 (40%) ps, respectively.

interactions influence all transitions because a pre-existing exciton generated by the pump beam shifts the excitation energy of the second exciton, whereas state filling, caused by population change in various electronic states following the initial pump-induced excitation, only disturbs the transitions involving the affected states. Therefore, existence of the common faster component in the bleaching recovery signals in Figure 4 indicates that it can be attributed to exciton−exciton interactions and the slower ones to state filling. Consequently, the slower time constants of 100 to 300 ps can be assigned to the lifetimes of the hot carriers in the discrete states probed, which are 2 orders of magnitude slower than those in bulk graphene or graphite and consistent with the expectation from the

© 2011 American Chemical Society

DOI: 10.1021/nl102712x | *Nano Lett.* **2011,** *11,* 56–60

discrete electronic states in the quantum dots. The time constant of the faster component should correspond to the lifetime of an electronic state (or states) that, through Columbic exciton−exciton interactions, affects all the states interrogated with the probe beams. We speculate that the state(s) should have higher excitation energy because of the shorter lifetime (18 ps), which nevertheless is also significantly longer than those in bulk materials, and greater density of states at higher energies. The red edge of state S_1 probed at 660 nm is the lowest excitonic and the fluorescence-emitting state. Its lifetime up to nanoseconds obtained with the transient absorption measurements is consistent with the fluorescence lifetime of **1**.[22] It is noted that exciton−exciton interaction should lead to induced absorption as well, which however is expected to appear out of the energy range that we have probed. Because of the size of quantum dot **1** and the small dielectric constant in graphene, we can estimate the first exciton generates an electric field of ∼1 V/nm within the quantum dots, which can shift the excitation energy of the second exciton by at least hundreds of electonvolts.

The energy spacing between initial and final states is an important parameter determining the rate of radiationless relaxation,[33,34] and therefore the rate of hot carrier relaxation depends on the density of states at the energy of the carriers. As a result, we expect that the lifetimes of hot carriers with higher energy could be significantly shorter than those of the discrete states probed in our studies,[35] and we speculate that the faster component in our TA spectra may be attributed to higher states. Similarly, the short induction periods of a few picoseconds in the TA traces could also be due to the shorter lifetimes of the states populated with the pump beam. This is consistent with the dramatically increased fluorescence intensity in the excitation spectrum when the quantum dots are excited to the continuum levels (wavelength shorter than 490 nm, Figure 2), suggesting faster and more efficient relaxation to reach the fluorescence-emitting state. The lifetimes of carriers in the continuum levels, as well as our assignment of the dynamic processes, will be investigated and further tested in future studies.

The slow hot-carrier relaxation in the graphene quantum dots makes it possible to reveal other normally slow relaxation pathways that are otherwise difficult to observe. For example, we have observed that intersystem crossing efficiently competes with internal conversion in **1**, so that the quantum dots emit not only fluorescence but also phosphorescence with relative intensities depending on excitation wavelengths.[22] Intersystem crossing is generally much slower than internal conversion since it involves a change in spin multiplicity. It can be enhanced in the graphene quantum dots due to the reduced singlet−triplet splitting in such a large conjugated system.[22] The prolonged lifetimes of hot carriers would further make it likely to be competitive against internal conversion. More interestingly, the reduced hot-carrier cooling rates could increase the efficiency of processes such as hot electron extraction or multiexciton generation to improve the efficiency of photovoltaic devices.[21,36] Excitons with energy in excess to the bandgap of semiconductors could be utilized through electron transfer or exciton multiplication before the excess energy is dissipated into heat and wasted.

Acknowledgment. We thank Professor John McGuire at Michigan State University for helpful discussions. This work was funded by the National Science Foundation (No. CBET-0747751), ACS Petroleum Research Fund (No. 47677-G10), and Indiana University.

Supporting Information Available. Time traces of transient absorption signals of **1** probed at 580 and 620 nm. This material is available free of charge via the Internet at http://pubs.acs.org.

REFERENCES AND NOTES

(1) Brus, L. E. *Appl. Phys. A* **1991**, *53*, 465–474.
(2) Efros, A. L.; Rosen, M. *Annu. Rev. Mater. Sci.* **2000**, *30*, 475–521.
(3) El-Sayed, M. A. *Acc. Chem. Res.* **2004**, *37*, 326–333.
(4) Nozik, A. J. *Annu. Rev. Phys. Chem.* **2001**, *52*, 193–231.
(5) Klimov, V. *J. Phys. Chem. B* **2000**, *104*, 6112–6123.
(6) Klimov, V. Charge Carrier Dynamics and Optical Gain in Nanocrystal Quantum Dots: From Fundamental Photophysics to Quantum Dot Lasing. In *Semiconductor and Metal Nanocrystals*; Klimov, V., Ed.; Marcel Dekker: New York, 2004; pp 159−214.
(7) Bockelmann, U.; Bastard, G. *Phys. Rev. B* **1990**, *42*, 8947–8951.
(8) Klimov, V.; McBranch, D. W. *Phys. Rev. Lett.* **1998**, *80*, 4028–4031.
(9) Pandey, A.; Guyot-Sionnest, P. *Science* **2008**, *322*, 929–932.
(10) Efros, A. L.; Kharchenko, V. A.; Rosen, M. *Solid State Commun.* **1995**, *93*, 281–284.
(11) Wang, L.-W.; Califano, M.; Zunger, A.; Franceschetti, A. *Phys. Rev. Lett.* **2003**, *91*, No. 056404.
(12) Cooney, R. R.; Sewall, S. L.; Anderson, K. E. H.; Dias, E. A.; Kambhampati, P. *Phys. Rev. Lett.* **2007**, *98*, 177403.
(13) Cooney, R. R.; Sewall, S. L.; Dias, E. A.; Sagar, D. M.; Anderson, K. E. H.; Kambhampati, P. *Phys. Rev. B* **2007**, *75*, 245311.
(14) Schroeter, D. F.; Griffiths, D. J.; Sercel, P. C. *Phys. Rev. B* **1996**, *54*, 1486–1489.
(15) Sercel, P. C. *Phys. Rev. B* **1995**, *51*, 14532–14541.
(16) Guyot-Sionnest, P.; Wehrenberg, B.; Yu, D. *J. Chem. Phys.* **2005**, *123*, No. 074709.
(17) Yan, X.; Cui, X.; Li, B.; Li, L.-S. *Nano Lett.* **2010**, *10*, 1869–1873.
(18) Yan, X.; Cui, X.; Li, L.-S. *J. Am. Chem. Soc.* **2010**, *132*, 5944–5945.
(19) Li, L.-S.; Yan, X. *J. Phys. Chem. Lett.* **2010**, *1*, 2572–2576.
(20) Geim, A. K. *Science* **2009**, *324* (5934), 1530–1534.
(21) Nozik, A. J. *Nano Lett.* **2010**, *10*, 2735–2741.
(22) Mueller, M. L.; Yan, X.; McGuire, J. A.; Li, L.-S. *Nano Lett.* **2010**, *10*, 2679–2682.
(23) Kampfrath, T.; Perfetti, L.; Schapper, F.; Frischkorn, C.; Wolf, M. *Phys. Rev. Lett.* **2005**, *95*, 187403.
(24) Breusing, M.; Ropers, C.; Elsaesser, T. *Phys. Rev. Lett.* **2009**, *102*, No. 086809.
(25) Dawlaty, J. M.; Shivaraman, S.; Chandrashekhar, M.; Rana, F.; Spencer, M. G. *Appl. Phys. Lett.* **2008**, *92*, No. 042116.
(26) Huang, L.; Hartland, G. V.; Chu, L.-Q.; Luxmi; Feenstra, R. M.; Lian, C; Tahy, K.; Xing, H. *Nano Lett.* **2010**, *10*, 1308–1313.
(27) Dresselhaus, M. S.; Dresselhaus, G.; Saito, R.; Jorio, A. *Annu. Rev. Phys. Chem.* **2007**, *58*, 719–747.
(28) Yang, L.; Cohen, M. L.; Louie, S. G. *Nano Lett.* **2007**, *7*, 3112–3115.

© 2011 American Chemical Society

DOI: 10.1021/nl102712x | *Nano Lett.* **2011,** *11,* 56–60

(29) Yang, L.; Deslippe, J.; Park, C.-H.; Cohen, M. L.; Louie, S. G. *Phys. Rev. Lett.* **2009**, *103*, 186802.
(30) Brus, L. E. *Nano Lett.* **2010**, *10*, 363–365.
(31) Ponomarenko, L. A.; Schedin, F.; Katsnelson, M. I.; Yang, R.; Hill, E. W.; Novoselov, K. S.; Geim, A. K. *Science* **2008**, *320* (5874), 356–358.
(32) Klimov, V. *Annu. Rev. Phys. Chem.* **2007**, *58*, 635–673.
(33) Henry, B. R.; Siebrand, W. Radiationless Transitions. In *Organic Molecular Photophysics*; Birks, J. B., Ed.; John Wiley & Sons: London, 1973; Vol. 1.
(34) Avouris, P.; Gelbart, W. M.; El-Sayed, M. A. *Chem. Rev.* **1977**, *77*, 793–833.
(35) Prezhdo, O. V. *Acc. Chem. Res.* **2009**, *42*, 2005–2016.
(36) Nozik, A. J. *Physica E* **2002**, *14*, 115–120.

© 2011 American Chemical Society

DOI: 10.1021/nl102712x | *Nano Lett.* **2011,** *11,* 56–-60